Developmental Biology 452 (2019) 83–94

Contents lists available at ScienceDirect

Developmental Biology

journal homepage: www.elsevier.com/locate/developmentalbiology

Lime is a new protein linking immunity and metabolism in *Drosophila*

Zorana Mihajlovic [a,b], Dajana Tanasic [a], Adam Bajgar [a,b], Raquel Perez-Gomez [a,b], Pavel Steffal [a], Alena Krejci [a,b,*]

[a] University of South Bohemia, Faculty of Science, Ceske Budejovice, Czech Republic
[b] Czech Academy of Sciences, Biology Centre, Institute of Entomology, Ceske Budejovice, Czech Republic

ARTICLE INFO

Keywords:
CG18446
Drosophila
Metabolism
Immunity
Leptopilina boulardii

ABSTRACT

The proliferation, differentiation and function of immune cells in vertebrates, as well as in the invertebrates, is regulated by distinct signalling pathways and crosstalk with systemic and cellular metabolism. We have identified the Lime gene (*Linking Immunity and Metabolism,* CG18446) as one such connecting factor, linking hemocyte development with systemic metabolism in *Drosophila*. Lime is expressed in larval plasmatocytes and the fat body and regulates immune cell type and number by influencing the size of hemocyte progenitor populations in the lymph gland and in circulation. Lime mutant larvae exhibit low levels of glycogen and trehalose energy reserves and they develop low number of hemocytes. The low number of hemocytes in Lime mutants can be rescued by Lime overexpression in the fat body. It is well known that immune cell metabolism is tightly regulated with the progress of infection and it must be supported by systemic metabolic changes. Here we demonstrate that Lime mutants fails to induce such systemic metabolic changes essential for the larval immune response. Indeed, Lime mutants are not able to sustain high numbers of circulating hemocytes and are compromised in the number of lamellocytes produced during immune system challenge, using a parasitic wasp infection model. We therefore propose the Lime gene as a novel functional link between systemic metabolism and *Drosophila* immunity.

1. Introduction

The development of immune cells, as well as their cellular and humoral response during an immune challenge, is tightly connected with dynamics in cell signalling (Man et al., 2017) (Vlisidou and Wood, 2015) coupled with changes in systemic and immune cell specific metabolism (Zmora et al., 2017) (Spiljar et al., 2017) (Buck et al., 2017). This includes the crosstalk between immune cells and adipose tissue (Mathis, 2013), liver (Jenne and Kubes, 2013), muscles (Yang and Hultmark, 2017) or microbiota in the gut (Levy et al., 2016). Functionally linking immune cell response with systemic metabolic changes is essential during immune challenge in both vertebrate and invertebrate species (Delmastro-Greenwood and Piganelli, 2013; Bajgar et al., 2015) and the detailed signalling pathways and transcriptional programmes involved in such inter organ communication are in the focus of intense current research.

The innate immune system of *Drosophila* is defined by the action of specific blood cells (hemocytes) and the expression of antimicrobial peptides (AMP) (Letourneau et al., 2016). The larval lymph gland (LG) represents one of the two main sites of active hematopoiesis in the fruit fly. Within the primary lobes of the LG, undifferentiated hemocytes progenitors (prohemocytes) reside in the medullary zone whereas differentiated immune cells, called plasmatocytes and crystal cells, reside in the cortical zone, with a narrow zone of intermediary progenitors in between these two zones (Krzemien et al., 2010). The posterior signalling centre (PSC) controls hemocyte differentiation (Krzemien et al., 2007), although its ablation does not affect prohemocyte maintenance (Benmimoun et al., 2015). Immune challenges lead to the specification of a third type of immune cell, found within the LG and circulation, called the lamellocyte (Rizki and Rizki, 1992) and causes the secretion of AMP (Coustau et al., 1996). The peripheral population of immune cells are comprised of those circulating in the fly hemolymph and the sessile cells that reside in another hematopoetic niche located between the epidermis and muscles, close the larval body wall (Leitao and Sucena, 2015). The majority of differentiated hemocytes in circulation, as well as in the lymph gland, are represented by plasmatocytes (conceptually related to mammalian macrophages), whilst crystal cells form a minority (Gold and Bruckner, 2014).

* Corresponding author. Current address: DT - Department of Cell and Molecular Biology, Medical Faculty Mannheim, University of Heidelberg, Germany.
E-mail addresses: vujin00@jcu.cz (Z. Mihajlovic), dajana.tanasic@yahoo.com (D. Tanasic), bajgaa07@prf.jcu.cz (A. Bajgar), perezgomezr@gmail.com (R. Perez-Gomez), steffp00@prf.jcu.cz (P. Steffal), akrejci@prf.jcu.cz (A. Krejci).

https://doi.org/10.1016/j.ydbio.2019.05.005
Received 31 August 2018; Received in revised form 6 May 2019; Accepted 6 May 2019
Available online 11 May 2019

The size of the LG, plus the number and type of cells in circulation, is determined by the nutritional status of the fly as well as by the activities of various signalling pathways and transcription factors, such as JAK/STAT, Hh, EGFR, Wg, PVR/STAT/ADGF or Hippo (Krzemien et al., 2010). During larval development the number of prohemocytes in the LG is controlled by signals from the PSC niche (Mandal et al., 2007) (Krzemien et al., 2007) (Sinenko et al., 2009), the pool of differentiated cells (Mondal et al., 2011) as well as by systemic insulin signalling and nutrient availability (Benmimoun et al., 2012) (Shim et al., 2012) (Okamoto et al., 2009).

Large proliferation of immune cells also occurs as a direct response to larval infection and is accompanied by differentiation of lamellocytes either from plasmatocytes or from lamelloblasts derived from prohemocytes (Anderl et al., 2016). Crystal cells do not play major role in this infection related process. The fat body, the *Drosophila* organ that is analogous to the adipose tissue and liver in vertebrates, is the key determinant of the immune response, as it is required to supply energy to sustain the immune system (DiAngelo et al., 2009). The immune response is energetically demanding and sufficient levels of nutrients need to be available to immune cells for successful immune defence (Buttgereit et al., 2000) (Straub et al., 2010). Accordingly, communication between the fat body and immune cells is bi-directional, with hemocytes being able to activate the Toll pathway in the fat body to produce AMP (Shia et al., 2009; Foley and O'Farrell, 2003) and *vice versa* (Schmid et al., 2014). In *Drosophila*, the immune response to wasp infection or to bacterial challenge activates the innate immune system and orchestrates a systemic metabolic switch that preferentially allocates energy to immune cells, mediated by adenosine release from hemocytes (Bajgar et al., 2015) or via activation of Mef-2 (Clark et al., 2013) and Toll signalling (Roth et al., 2018) in the fat body.

In this work, we have identified the Lime gene (CG18446) as a new player in mediating crosstalk between the immune system and systemic metabolism in *Drosophila*. We show that Lime controls the development of the immune system by affecting the number of undifferentiated hemocyte progenitors but it is also important for the regulation of energy stores of glycogen and trehalose that can reciprocally affect hemocyte development and function. The Lime mutant fails to induce the systemic metabolic changes essential for mounting/sustaining successful immune defence and it is compromised in the generation of circulating immune cells, including the specification of lamellocytes necessary for the defence against a parasitic wasp intruder. In summary, Lime is a new functional link between metabolism and *Drosophila* immunity.

2. Methods

2.1. Generation of Lime (CG18446) alleles and expression constructs

The Lime^{exD} allele was generated using recombination between two Exelixis transposons, the *P{XP}CG46338^{d07017}* and *PBac{RB}CG46338^{e00513}*. The stocks were first cleaned from potential floating mutations by crossing six times to isogenized w^{1118} Exelixis stock and the XP and RB transposons were recombined by the induction of hs-FLP (Thibault et al., 2004). The resulting 5 kb deletion includes the Lime gene, *lncRNA:CR45138* and one of the promoters for *CG46338*.

The Lime-*Flyfos-GFP* flies were created by specific integration of the 42 kb transgenic BAC clone 9358301918258116_G08 obtained from Mihail Sarov (Sarov et al., 2016) into the attP50 site on chromosome 2R. Lime is driven by its endogenous promoter within the context of the BAC clone and it is tagged with C-terminal GFP (https://transgeneome.mpi-cbg.de/transgeneomics/public/clone.html?wellId=59886725). The Lime-Flyfos-GFP expression pattern in the embryo is very similar to the *in situ* data deposited in the BDGP database (Fig. S1).

The *UAS*-Lime-GFP construct was generated by cloning the Lime ORF with C-terminal GFP tag into the pUASt plasmid and specific integration into *attP40* site.

The *Srp-Gal4, UAS-Gal80^{ts}* flies were obtained from Michele Crozatier and larvae were shifted from 25 °C to 29 °C 24 h after egg laying to activate the Gal4 driver. The *HmlΔ-Gal4* stock was a gift from Bruno Lemaitre (Sinenko and Mathey-Prevot, 2004).

All flies were raised on a diet consisting of 8% cornmeal, 5% glucose, 4% yeast and 1% agar.

2.2. Hemocyte quantification, immunostaining and antibodies used

To calculate the number of circulating hemocytes in the hemolymph, >15 larvae per genotype were washed gently in PBS, bled individually into 13ul PBS and the number of cells calculated on Neubauer improved counting chamber (Sigma), under the light microscope. In case of infection, lamellocytes were distinguished by differential interference contrast (DIC) adjustment; only the large and completely flat cells were scored as mature lamellocytes.

Lymph glands from late L3 larvae were dissected in PBS, fixed in 4% formaldehyde in PBS for 30 min, washed three times with PBS - 1% Triton X100, incubated with primary antibodies overnight (1:100), washed three times with PBS - 1% Triton X100 and incubated with secondary antibodies (1:500) for 1 h, followed by three washes with PBS - 1% Triton X100 and DAPI. Tissue was mounted in Aqua Polymount (Polysciences) and imaged on Olympus IX81 Confocal Laser Scanning Microscope. Identical (and non-saturating) laser and confocal settings were used throughout a single experiment that included control and experimental samples. Quantification of signal intensities was performed by Olympus FluoView FV1000 or ImageJ software. Volumes of lymph glands were measured in Imaris software (Bitplane).

For immunostaining of circulating hemocytes individual L3 larvae were bled into 20 µl *Schneider* media, the drop was then transferred to a coverslip and cells were left to attach for 30 min in a humidified chamber, fixed for 20 min in 2% formaldehyde in PBS before application of the standard immunostaining protocol (see above). For quantification of the percentage of *P1*$^{+}$ cells in the hemolymph, confocal pictures from three random locations in the drop were selected and the percentage of *P1*$^{+}$ cells calculated, with 10–20 larvae per genotype. For quantification of crystal cells in the hemolymph, immunostaining was performed with an α-Hnt antibody and the total number of Hnt^{+} cells counted under a fluorescence microscope (Olympus). Colocalization on polytene chromosomes was performed according to previously described protocols (Corona et al., 2004).

For the immunostaining of Lime-Flyfos-GFP in embryos, staged embryos were collected from agar plates, washed with PBS, dechorionated in 100% bleach for 2 min and fixed in 4% formaldehyde in PBS and heptane (1:1 mix) for 15 min. The lower phase of the fix solution was removed and embryos were then vortexed for 2 min in methanol to remove the extraembryonic membranes. After rehydratation in PBT, the standard immunostaining protocol (see above) using the α-GFP antibody was applied.

The following antibodies were used: α -P1 (gift from I. Ando), α-Lz (DSHB), α-Hnt (DSHB), α-Ant (DSHB), α-phosphorylated Ser2 and Ser5 CTD of RNA PolII (Abcam ab5408), α-GFP (ThermoFisher G10362).

2.3. Infection of larvae with the wasp Leptopilina boulardii

Flies were permitted to lay eggs on cornmeal medium at 25 °C for 4 h, after which eggs were further incubated for 72 h at 25 °C. One hundred and twenty larvae were then carefully transferred to fresh food and combined with 100 female wasps for 1 h in the dark, resulting in a strong infection with an average of more than 5 eggs per larva. The infected and control non-infected larvae were kept at 25 °C until cell counting was performed. To assess the survival rate, larvae from 5 independent infection experiments were kept at 25 °C and the number of emerging adults were counted after hatching.

2.4. RNA extraction and quantification

The larval fat bodies (10 larvae), guts (10 larvae), wing discs (30 larvae) were dissected in PBS at room temperature over the time course of 10 min, transferred immediately into ice cold PBS, spun, resuspended in 0.5 ml Trizol (Sigma) and RNA extracted according to the manufacturer's protocol. RNA was treated with DNAse (*DNA Free* reagent from Ambion), 1 μg of RNA was reverse transcribed with M-MLV reverse transcriptase (Sigma), and specific cDNAs (mRNAs) were quantified by real time PCR using GoTaq qPCR master mix (Eastport Scientific) run on a BioRad CFX96 machine. For mRNA isolation from hemocytes, 30 larvae were bled in PBS, and the hemocytes were spun in a microcentriguge with the resulting pellet being resuspended in Trizol prior to cDNA synthesis (described above). Primers were designed not to span introns, and a calibration curve from serially diluted genomic DNA was used in every run to accurately quantify the cDNA. Specific gene transcript levels were normalized to those of the rp49 gene. The primer sequences used for Lime mRNA quantifications were GCTGGTCAAGGAGATTCTGG and CATGTTGGGTGAGGTGCTC; and for rp49 CCGCTTCAAGGGACAGTATC and TTCTGCATGAGCAGGACCTC.

2.5. Metabolite measurement

After 24 h of infection (96 h after egg laying), larvae were washed in PBS and in water before the hemolymph was collected on ice to prevent melanisation. In the cases of whole body metabolite measurements, whole larvae were homogenized in ice cold PBS, spun in order to get rid of larval debris with the resulting supernatant being collected for subsequent measurements. Glucose, trehalose, and glycogen were measured as previously described (Tennessen et al., 2014), employing the GAGO-20 kit (Sigma) and derived values were normalized to total protein content in the hemolymph or larvae, respectively. Twenty larvae of each genotype and condition were used for hemolymph measurements and five larvae for the whole body measurements, in each replicate. For HPLC/ESI/MS analysis lipids were extracted via a previously described chloroform and methanol solution based methodology (Folch et al., 1957) and analyzed with ion trap LTQ mass spectrometer coupled to a Surveyor HPLC system equipped with Acela autosampler (all by Thermo,

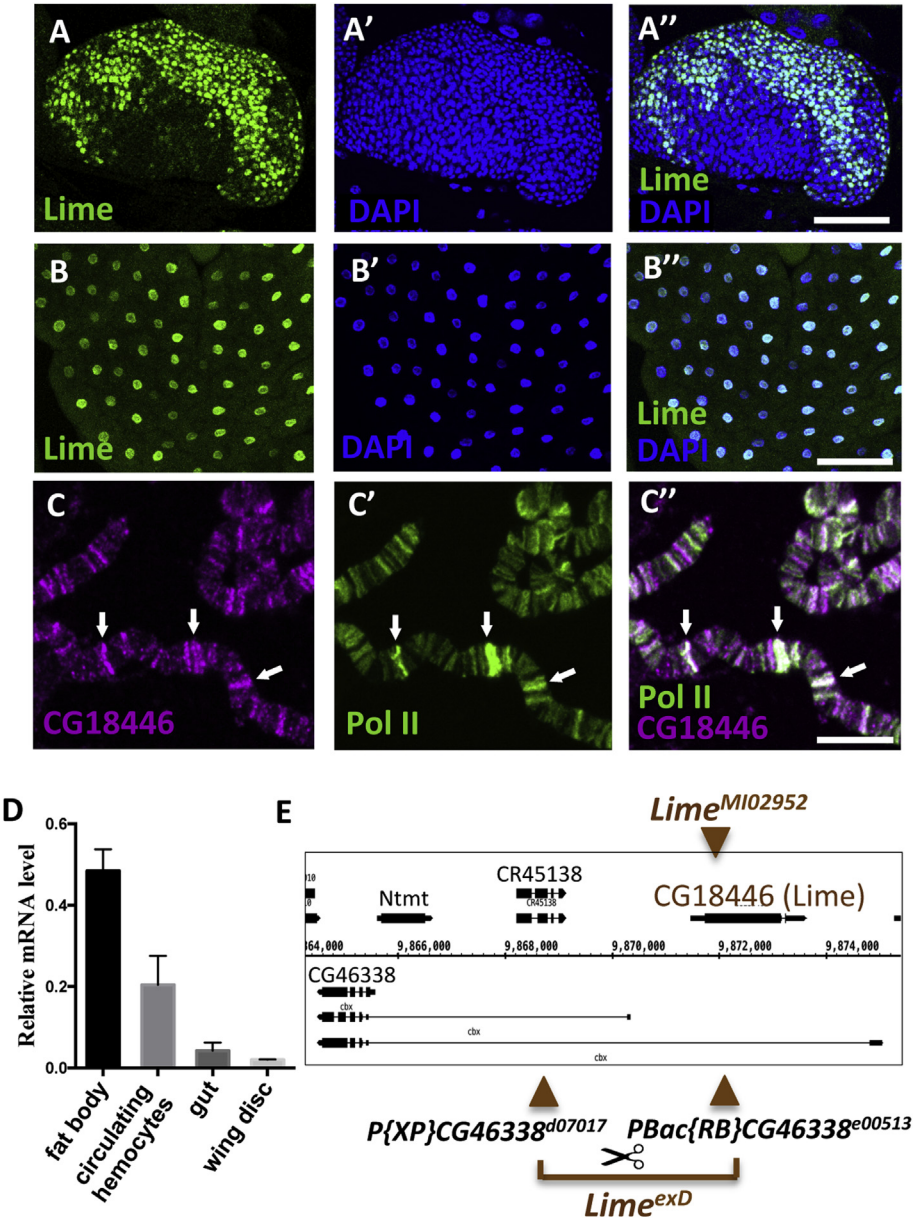

Fig. 1. Lime (CG18446) is a nuclear protein expressed in immune cells and fat body tissue. A. GFP immunostaining of the *Lime-Flyfos-GFP* (green) in the late L3 larval lymph gland. Scale bar 50 μm. B. GFP immunostaining of the *Lime-Flyfos-GFP* (green) in the late L3 larval fat body. Scale bar 100 μm. C. Polytene chromosomes of *patched-Gal4>UAS-Lime-GFP* flies stained against GFP (magenta) and phosphorylated Ser2/Ser5 CTD of RNA polymerase II (*PolII*, green). Arrows point to several examples of overlapping bands. Scale bar 5 μm. D. Quantification of endogenous *Lime* mRNA in selected tissues of late L3 larva. Mean with standard error of the mean from 3 biological replicates. E. Genomic location of the $Lime^{MI02952}$ and $Lime^{exD}$ alleles.

San Jose, CA, USA). The samples (5 µl) were injected and separated using the Gemini column 250 × 2 mm i.d. 3 µm (Phenomenex, Torrance, CA, USA) according to (Schneedorferova et al., 2015). Peak areas of detected lipids were used for the estimation of their relative content in the analyzed samples.

2.6. Quantification and statistics

For the hemocyte counts and immunostaining, 15–52 larvae were analyzed for each genotype and condition per biological replicate. Lymph gland immunostaining quantification was based on average signal intensities from >10 lymph glands. Similarly, 10 lymph glands were used for average volume measurements. For metabolite measurements, hemolymph was pooled from 20 larvae and 5 larvae were used for whole body metabolite extraction. RNA was isolated from fat bodies of 10 larvae for each genotype and experimental condition, per biological replicate. Infection was performed with 120 larvae of indicated genotype per biological replicate. The scatter plot graphs represent means with 95% confidence interval, except Figs. 6A, 6B, S2C and S2B where the standard error of the mean is plotted. Student's t-test was used to compare individual treatments. *p ≤ 0.05; **p ≤ 0.01; ***p ≤ 0.001.

3. Results

We identified the CG18446 gene as being expressed in the larval lymph gland (LG), in circulating hemocytes and in the fat body of *Drosophila* (Fig. 1A, B, 6D). It encodes a small protein of 384 amino acids that comprises three C_2H_2 type Zn-finger domains and has a putative nuclear localization signal at its N-terminal; indeed, a GFP-tagged protein product, expressed from the endogenous gene promoter in the Flyfos transgene, localizes to the nucleus (Figs. 1A and 6D). Immunostaining of the GFP fusion protein on the polytene chromosomes of the salivary glands reports association of CG18446 at sites of active transcription, based on its co-localization with the actively transcribing RNA polymerase II (phosphorylated at Ser2 and Ser5 in the CTD domain - Fig. 1C). To date the function of CG18446 gene has not been described but it is known that its transcription depends on multiple retro element insertions within the promoter regions (Merenciano et al., 2016) and may involve active Notch signalling (Housden et al., 2013) (Krejci et al., 2009). Based on the expression pattern of CG18446 and the phenotypes described in this paper, we decided to name the gene Lime, as an acronym for Linking Immunity and Metabolism.

In order to characterize a Lime mutant phenotype, we created the $Lime^{exD}$ allele comprising a small 5 kb deletion, generated by the FRT mediated recombination of two Exelixis transposons (Thibault et al., 2004) that removed the entire coding sequence of the Lime gene, *lncRNA:CR45138* and one of the promoters of *CG46338* gene (Fig. 1E). We also employed the $CG18446^{MI02952}$ allele, in which a mimic transposon was inserted straight after the beginning of the Lime open reading frame (Venken et al., 2011). To characterize the Lime mutant phenotypes we crossed the $y^1\ w^{1118}$; $Lime^{MI02952}$ with w^{1118};$Lime^{exD}$ flies and analyzed the transheterozygous $Lime^{MI02952}/Lime^{exD}$ progeny, in comparison to

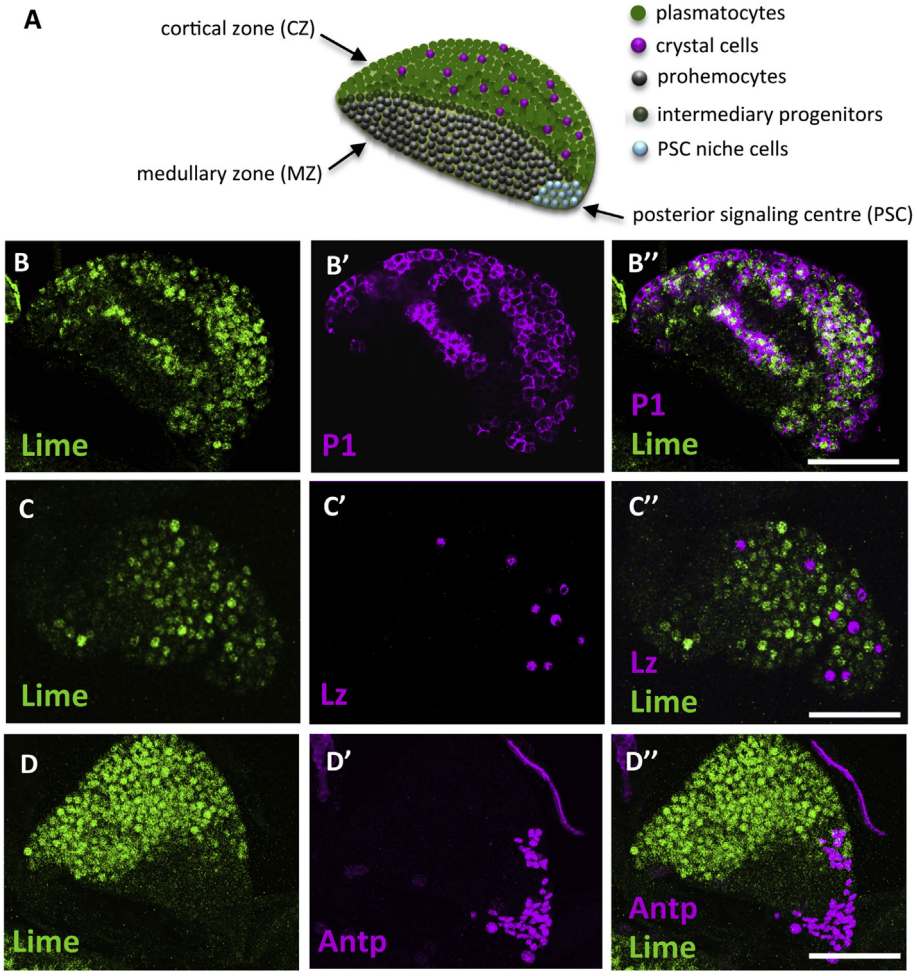

Fig. 2. Lime expression colocalizes with plasmatocytes in the lymph gland. A. Schematic representation of the late L3 larval lymph gland and its cell subtypes. *B. Lime-Flyfos-GFP* flies stained with GFP (green) and with the marker of plasmatocytes (*P1*, magenta). *C. Lime-Flyfos-GFP* flies stained with GFP (green) and with the marker of crystal cells (*Lozenge*, *Lz*, magenta). *D. Lime-Flyfos-GFP* flies stained with GFP (green) and with the marker of PSC cells (*Antennapedia*, *Antp*, magenta).

control progeny from y^1 w^{1118} flies crossed to w^{1118}. Although it should be noted that we also verified the key identified phenotypes in the transheterozygous larvae (see bellow) with larvae homozygous for $Lime^{MI02952}$ *or* $Lime^{exD}$ (Fig. S2).

3.1. *Lime affects the development of immune cell populations by regulating the number of prohemocytes*

We first decided to characterize the role of Lime in the development of the *Drosophila* larva immune system. We detected Lime expression in the cortical zone of the late L3 lymph gland, where it colocalized with plasmatocyte marker (P1) but not those specific for crystal cells (Hnt or Lz). We did also observe some scattered Lime positive and Hnt negative cells in the medullary zone but not in the posterior signalling centre (PSC) (Fig. 2B–D). Moreover, it was obvious that the lymph gland of mutant flies were significantly smaller than controls (Fig. 3A, B, C); accordingly, there were fewer plasmatocytes ($P1^+$) and crystal cell (Hnt^+) present. However, when the P1 signal was normalized to the volume of the lymph gland, the plasmatocyte density within the tissue was similar to controls (Fig. 3C). This suggests that the smaller size of the lymph gland is not caused by a simple lack of differentiated cells in the cortical zone but the number of prohemocytes in the medullar zone is also smaller. The same downward trends were observed in the circulating immune cells in the hemolymph of Lime mutant. Indeed, the Lime mutant had fewer cells in circulation and contained fewer plasmatocytes ($P1^+$) as well as crystal cells (Hnt^+), but the percentage of P1 positive cells, relative to the total, was similar to controls (Fig. 3D). There were also trends reflecting an increased percentage contribution of differentiated cells ($P1^+$ or Hnt^+) and a smaller pool of undifferentiated prohemocytes ($P1^-$, Hnt^-) (Fig. 5A). Although crystal cells normally represent only a minor pool of immune cells in both the lymph gland and in circulation, their differentiation was negatively affected in the Lime mutant (Fig. 3C, D). We concluded that the Lime gene is important for establishing sufficient numbers of immune cells, both in the lymph gland and in circulation.

As Lime is expressed in immune cells as well as in the fat body, we assayed for Lime over-expression phenotypes using a *Serpent-Gal4* driver (*Srp-Gal4*) that is active in both of these tissues. Consistent with the incidence of small lymph glands in Lime mutant, we observed large overgrowth of the lymph glands after Lime gene over-expression (Fig. 4A–C). The overgrowth was caused mainly by the expansion of undifferentiated prohemocytes ($P1^-$, Hnt^-) because there were fewer differentiated plasmatocytes ($P1^+$) and crystal cells (Hnt^+) when normalized to the overall volume of lymph gland (Fig. 4C). Similar results, with even more profound phenotypes, were observed in the pool of circulating cells in the hemolymph (Fig. 4D). Indeed, such larvae presented with many more immune cells in circulation (in extreme cases up to 40x more than controls), the majority of which (94%) were comprised of undifferentiated prohemocytes ($P1^-$, Hnt^-) (Fig. 5A and B). Based on these combined mutant and over-expression phenotypes, we conclude that Lime regulates the number of prohemocytes (immune cell progenitors) in *Drosophila* larva, both in the lymph gland and in circulation.

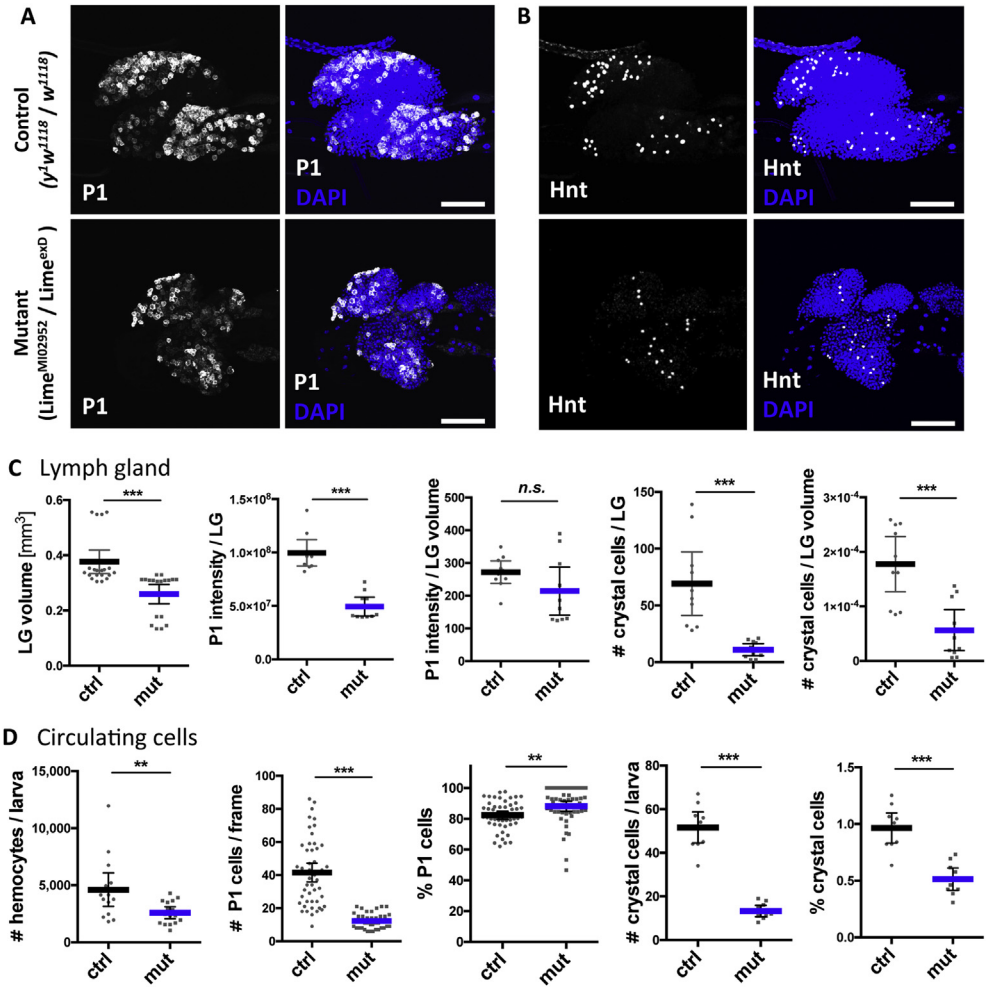

Fig. 3. Lime mutant develops fewer immune cells. A., B. Immunostaining of plasmatocyte marker (P1, in white) and crystal cell marker (Hindsight, Hnt, in white) in the L3 lymph glands of Lime mutant ($Lime^{MI02952}/Lime^{exD}$) and control ($y^1w^{1118}/w^{1118}$). Mutant lymph glands are smaller than controls. Scale bar 50 μm. C. Quantification of lymph gland volume, P1 and Hnt signals of lymph glands stained in experiments in A and B. Mean with 95% confidence interval. D. Quantification of total number of circulating hemocytes and the signal from immunostaining against plasmatocyte marker (P1) and crystal cell marker (*Hnt*) in *Lime* mutant ($Lime^{MI02952}/Lime^{exD}$, in blue) and control ($y^1w^{1118}/w^{1118}$, *in* black). Mean with 95% confidence interval. Data in C and D are based on quantification of 10–20 larvae per genotype.

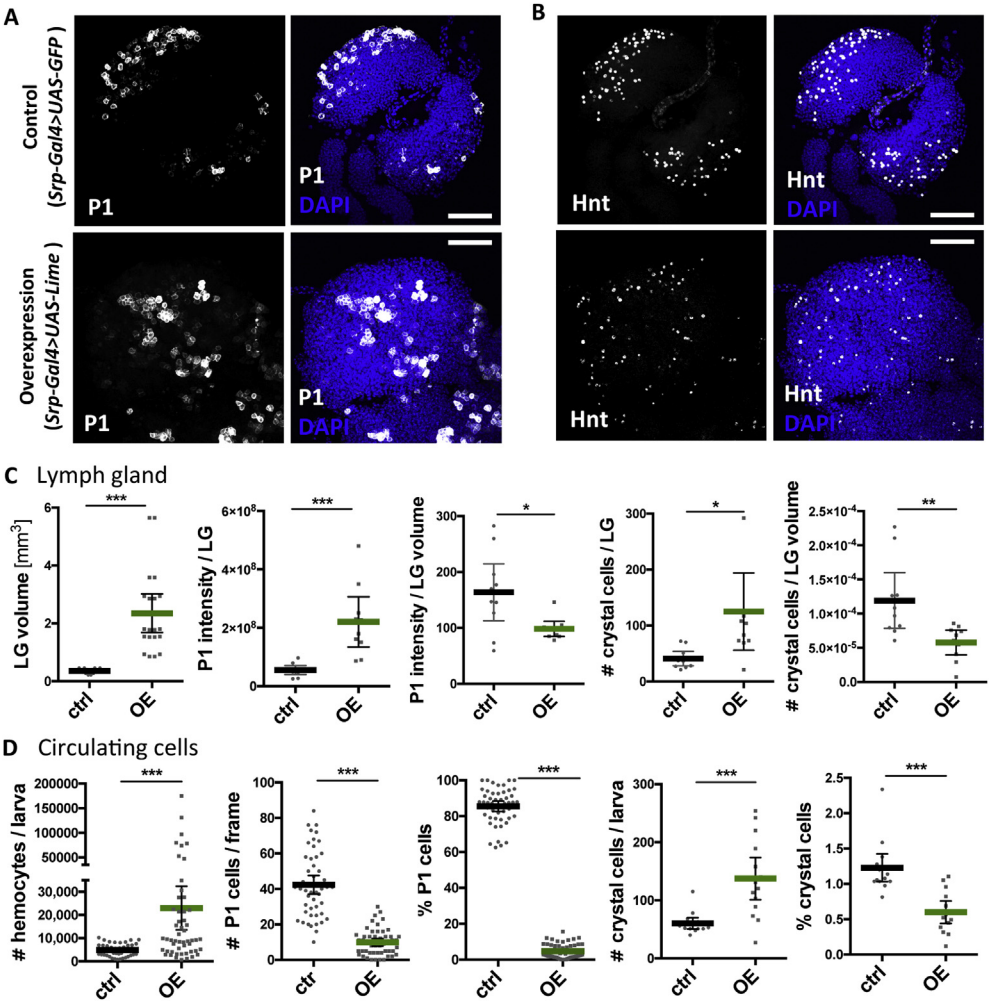

Fig. 4. Lime overexpression in immune cells and fat body using *Srp-Gal4* driver leads to overproliferation of undifferentiated prohemocytes. A., B. Immunostaining of the plasmatocyte marker (P1, white) and crystal cell marker (Hnt, white) in the L3 lymph glands of *Srp-Gal4, UAS-Gal80^{ts} > UAS-Lime* flies (OE, overexpression) *and Srp-Gal4, UAS-Gal80^{ts} > UAS-GFP* (control). Lymph glands with *Lime* overexpression are bigger than controls, only one lobe is shown. Scale bar 50 μm. C. Quantification of lymph gland volume, P1 and Hnt signal of lymph glands stained in experiments in A and B. Mean with 95% confidence interval. D. Quantification of total number of circulating hemocytes and the signal from immunostaining of plasmatocyte marker (P1) and crystal cell marker (Hnt) in circulating cells of Srp-Gal4, *UAS-Gal80^{ts} > UAS-Lime* flies (green) and controls (*Srp-Gal4, UAS-Gal80^{ts} > UAS-GFP,* in black). Mean with 95% confidence interval. Data in C and D are based on quantification of 10–50 larvae per genotype.

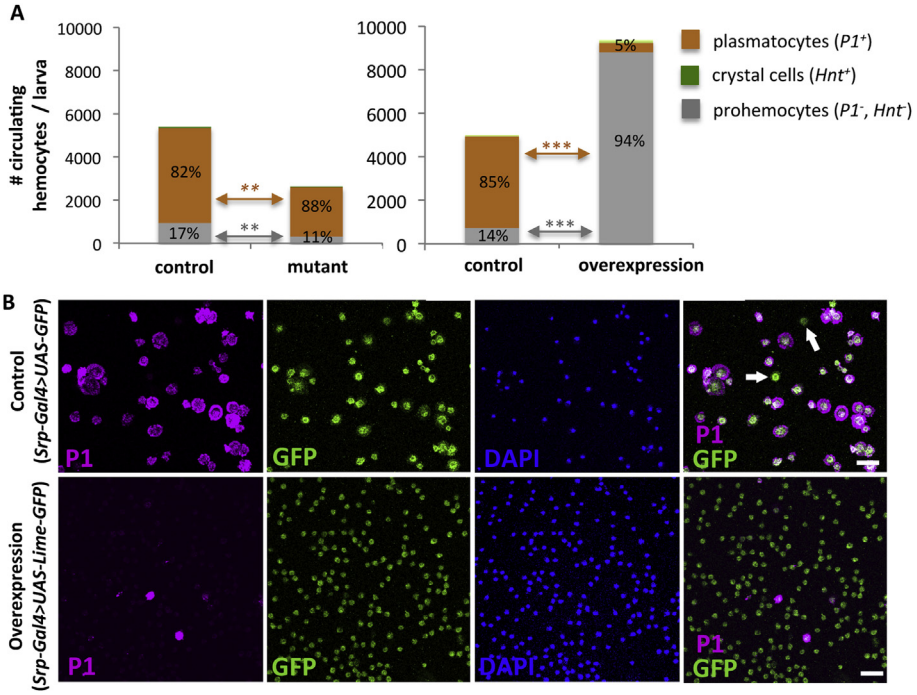

Fig. 5. Lime regulates the pool of undifferentiated prohemocytes in circulation. A. Average number of circulating plasmatocytes (P1^{+}), crystal cells (Hnt $^{+}$) and prohemocytes (P1^{-}, Hnt $^{-}$) per larva in Lime mutant (*Lime^{MI02952}/Lime^{exD}*) and control (*y^{1}w^{1118}/w^{1118}*) and after Lime overexpression in circulating hemocyte and fat body (*Srp-Gal4, UAS-Gal80^{ts} > UAS-Lime*) and in control (*Srp-Gal4, UAS-Gal80^{ts} > UAS-GFP*). Based on data shown in Figs. 3D and 4D. B. Immunostaining of circulating hemocytes in L3 larvae with Lime overexpression in circulating hemocyte and fat body (*Srp-Gal4, UAS-Gal80^{ts} > UAS-Lime-GFP*) and in control (*Srp-Gal4, UAS-Gal80^{ts} > UAS-GFP*). The P1 (magenta) negative cells prevail amongst the overproliferated hemocytes (labelled by GFP in green). The GFP signal is cytoplasmic in control and nuclear in the overexpression larvae. White arrows point to the small number of P1 negative hemocytes in controls. Scale bar 20 μm.

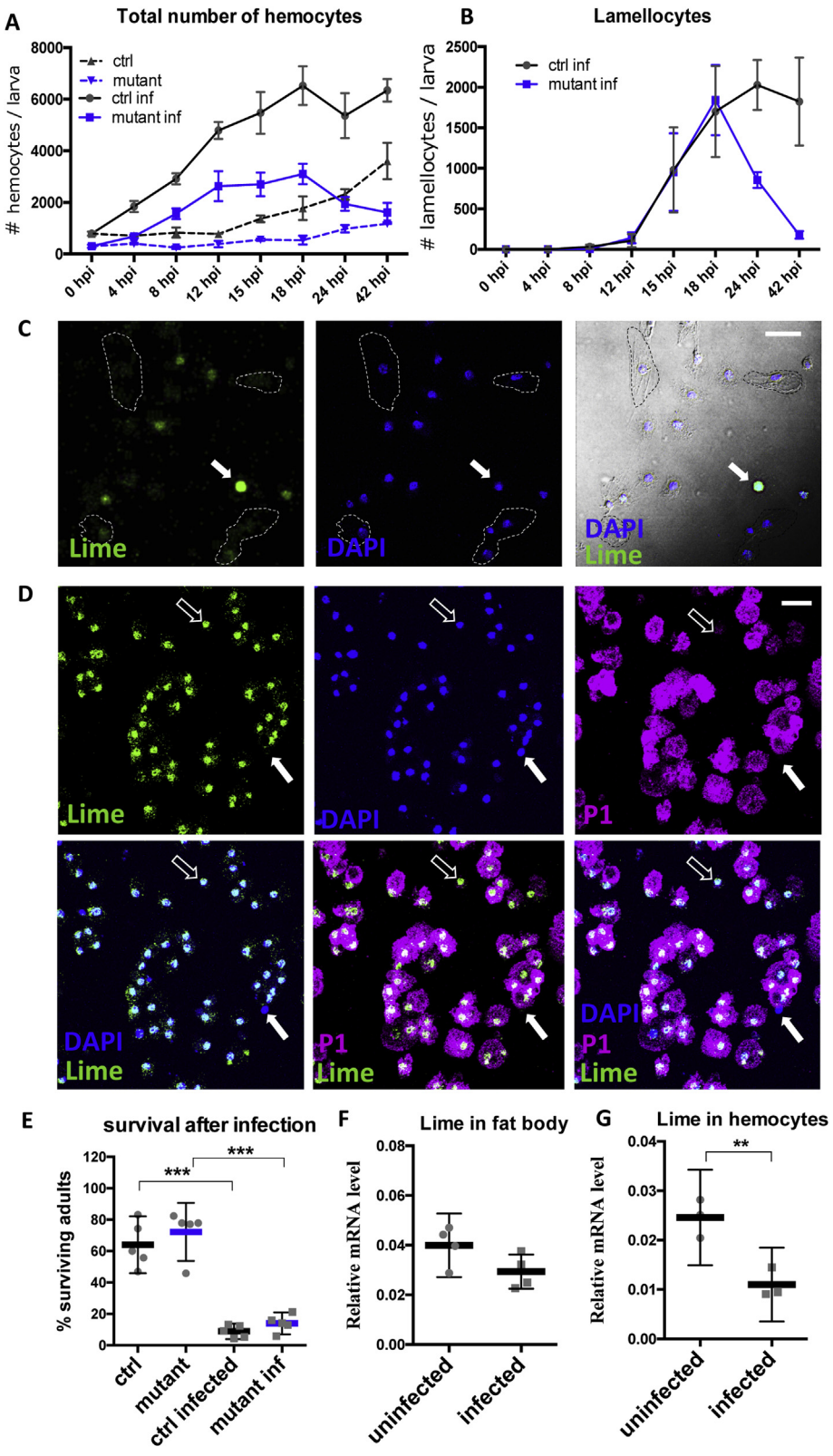

Fig. 6. Lime mutant fails to achieve sufficient numbers of circulating hemocytes, including lamellocytes, during wasp infection. A. Total number of circulating immune cells in *Lime* mutant ($Lime^{MI02952}$/$Lime^{exD}$, in blue) and controls (y^1w^{1118}/w^{1118}, in black) in time intervals up to 42 h post-infection (hpi) of larvae with the parasitic wasp *Leptopilina boulardii*. Inf - infected. Mean with SEM from 3 biological replicates. B. Number of circulating lamellocytes in *Lime* mutant and control larvae in time intervals up to 42 h after wasp infection. Mean with SEM from 3 biological replicates. C. Mature lamellocytes do not express *Lime*. Immunostaining of the GFP signal in *Lime-FlyFos-GFP* circulating hemocytes 24 h after wasp infection. Mature lamellocytes are marked by dashed line, arrow points to GFP strongly positive plasmatocyte. Scale bar 20 μm. D. All plasmatocytes (P1, magenta) express Lime (GFP, green) in *Lime-FlyFos-GFP* larvae without the immune challenge. There are rare cases of Lime positive hemocytes that do not express P1 (empty arrow) as well as hemocytes that do not express Lime nor P1 (full arrow). Scale bar 20 μm. E. Percentage of control and mutant larvae that developed to adult flies after the wasp infection. Mean with 95% confidence interval from 5 biological replicates. F. Quantification of mRNA expression of Lime in the fat body 24 h after wasp infection of y^1w^{1118} control larvae. Mean with 95% confidence interval from 4 biological replicates. G. Quantification of mRNA expression of Lime in circulating hemocytes 24 h after wasp infection of y^1w^{1118} control larvae. Mean with 95% confidence interval from 3 biological replicates.

3.2. *Lime mutants have low numbers of circulating lamellocytes during later stages of immune response*

As immune cell numbers were compromised in the Lime mutant, we decided to test if this would affect the mutant's response to an immune challenge. Accordingly, we infected *Drosophila* larvae with the parasitic wasp *Leptopilina boulardii* and analyzed the number of circulating hemocytes in time intervals up to 42 h post-infection. As expected, the number of circulating hemocytes at the beginning of the infection was already compromised at the start of the infection, however these lower levels did begin to increase at a similar rate as observed in controls, up until 12 h after infection. However, whilst hemocyte proliferation

continued in control larvae, the initial increase in hemocyte numbers in Lime mutants was followed by a plateau phase and eventually a decrease from a point some 18 h post infection (Fig. 6A). At the 12 h post-infection time point, it was possible to observe the appearance of lamellocytes (required to neutralise the wasp egg by melanisation). Despite having fewer initial circulating immune cells, the Lime mutant was able to produce an equivalent number of lamellocytes as control larvae up to 18 h after infection (Fig. 6B). However, it was not able to further maintain lamellocyte production and the number of lamellocytes dropped sharply by 42 h after infection (Fig. 6B). We were able to rescue this phenotype, using the Lime-*Flyfos-GFP* construct (Fig. S3), suggesting that the phenotype is indeed Lime specific. Despite the low number of lamellocytes in later stages of infection, the Lime mutant did not show any differences in the larva survival rate (Fig. 6E).

Interestingly, the expression of Lime mRNA within the fat body of parasitized control larvae was not significantly changed compared to non-infected groups (Fig. 6F). These results indicate that the transcription of the Lime gene is not affected during the immune challenge, but they do not exclude the possibility that Lime protein activity could be regulated on a post-transcriptional level. Such type of post-transcriptional regulation it the fat body has been described with Mef2 immune-metabolic switch (Clark et al., 2013). We did however observe a significant decrease in Lime mRNA levels in isolates of circulating hemocytes after infection (Fig. 6G). To distinguish in which cell type Lime expression was decreased, we performed immunostaining of Lime-Flyfos-GFP in circulating hemocytes, both before and after wasp infection. Before the wasp infection Lime was expressed in all circulating P1 positive hemocytes, although a scattered signal could also be detected in some of the P1 negative cells (Fig. 6D); a result similar to that observed in the lymph gland (Fig. 2B). After the wasp infection Lime signal was gradually lost as cells started to form flat processes (plasmatocytes differentiating into lamellocytes) and it was completely absent in mature lamellocytes (Fig. 6C). Thus, the decrease in Lime mRNA expression within the pool of circulating hemocytes post infections can most probably be explained by the expansion of Lime negative lamellocytes during the immune challenge.

3.3. *Lime mutants larvae fail to maintain energy levels and elicit systemic metabolic changes essential for immune response*

The fat body is a central regulator of overall energy metabolism in the fly; storing triglycerides and glycogen as energy resources (Zhang and Xi, 2015). Stored glycogen can be converted to trehalose and subsequently to glucose to be released into the circulating hemolymph, as a response of the organism's need for energy (Yamada et al., 2018). During the mobilization of fatty acids, triglycerides (TG) in the fat body are converted to diglycerides (DG) that are released to the hemolyph (Arrese and Wells, 1997). Under normal conditions, trehalose represents the main circulating carbohydrate in the fly hemolymph and it is transported to peripheral tissues to be converted into two glucose molecules that can sustain glycolysis. Therefore, glucose levels under such normal conditions are low within the hemolymph but it is essential that they rise

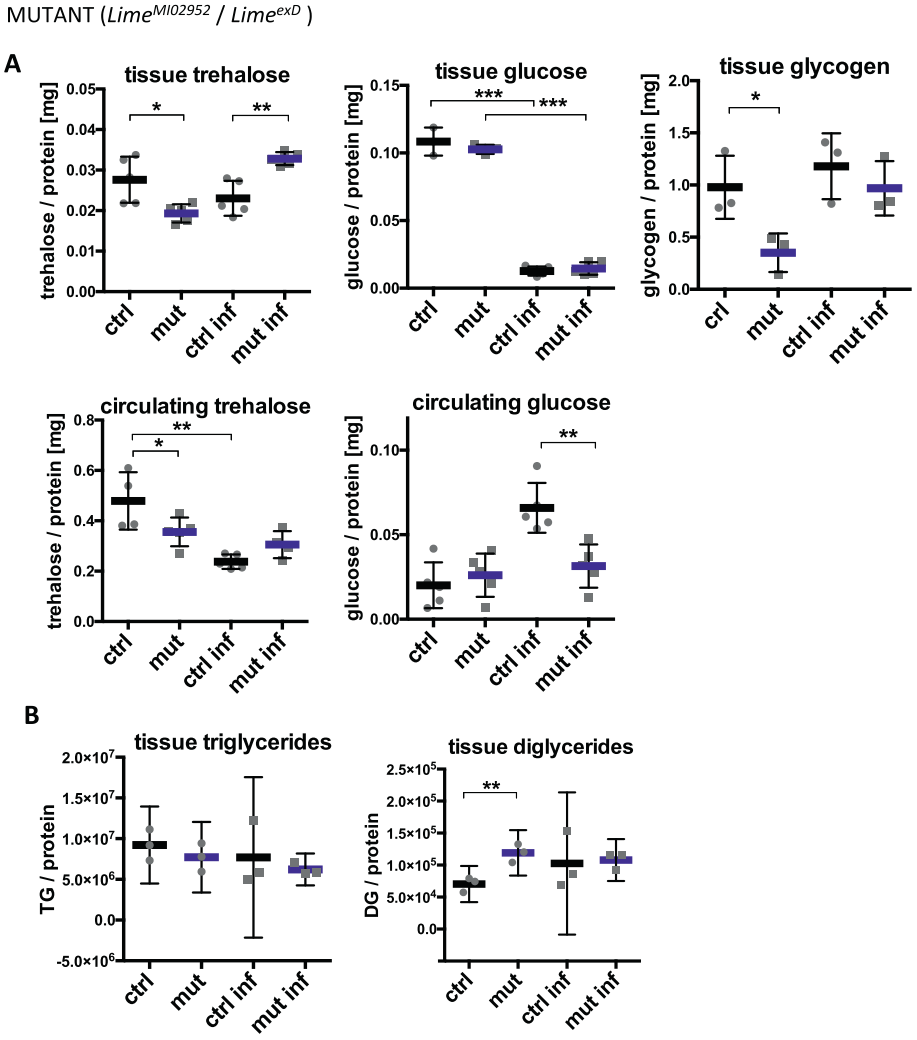

Fig. 7. Lime mutant has low energy reserves and fails to induce metabolic response after wasp infection. A. Analysis of trehalose, glucose and glycogen concentrations in the whole larva and in the hemolymph of *Lime* mutant (*Lime*^{MI02952}/*Lime*^{exD}, in blue) and control (y^1w^{1118}/w^{1118}, in black) 24 h after wasp infection (inf), 96 h after egg laying. Mean with 95% confidence interval with data points obtained from two biological replicates. B. Analysis of trilyceride (TG) and diglyceride (DG) levels in the whole larva of mutant and control 24 h after wasp infection (inf), 96 h after egg laying. Mean with 95% confidence interval from 3 biological replicates.

during an immune challenge, in order to support the development and function of the immune system (Bajgar et al., 2015). The fat body is indispensable in executing this role, as it supplies the excess of energy required for the activation of immune cells (Bajgar et al., 2015).

As we discovered Lime is expressed in the fat body (Fig. 1B) we investigated whether Lime mutants would display any metabolic phenotypes. Indeed, we found that Lime mutant larvae have lower levels of tissue glycogen and trehalose, the two main energy storing carbohydrate molecules in the fly (Fig. 7A). The levels of circulating trehalose were also lower, although it was enough to maintain the basal levels of circulating glucose to a degree similar to control larvae. It is known that triglycerides are by mass the main energy reserve for the fly. Triglycerides are deposited mainly in the fat body and are cleaved by various lipases to yield di- and mono-glycerides during lipolysis (Kuhnlein, 2012). In the Lime mutant larvae, we did not observe a statistically significant difference in the levels of triglycerides, although the average value in mutant was lower than the average value in control (Fig. 7B). However, we detected significantly higher levels of diglycerides (Fig. 7B), suggesting that lipolysis is increased in Lime mutant. The uncovered perturbations in carbohydrate and lipid metabolites are consistent with a metabolic regulatory role for Lime, most probably via the fat body; although as we assayed the levels of such metabolites in the whole larvae we cannot exclude the potential involvement of other tissues.

Complementing the metabolic data from Lime mutant, we also observed reciprocal increases in circulating and tissue trehalose levels, plus elevated levels of circulating glucose in larvae in which the Lime gene had been over-expressed with the *Srp-Gal4* driver (Fig. 8).

During wasp infection, hemolymph glucose represents the main energy source for immune cells and up-regulation of circulting glucose levels in the hemolymph is essential for the development of a successful immune response (Bajgar et al., 2015). Strikingly, the Lime mutant fails to up-regulate circulating glucose levels during wasp infection; probably because the levels of trehalose and glycogen are already low before the infection (Fig. 7A). Indeed, the elevated levels of tissue trehalose and glycogen we observed in Lime mutants during infection suggest an active deprivation of energy provision to circulating hemocytes in favour of increased energy storage (Fig. 7A).

3.4. Lime in the fat body increases the total number of larval hemocytes

As Lime is expressed in both embryonic and larval hemocytes as well as in the fat body, we wanted to initiate investigation into potential tissue specific effects of Lime expression on hemocyte development. When we over-expressed Lime in the fat body, using the *FB-Gal4* or *C7-Gal4* drivers, we observed an increased number of circulating hemocytes and morphologically larger lymph glands (Fig. 9A and B). Conversely, the over-expression of Lime in differentiated hemocytes (not in prohemocytes), employing the *Hml-Gal4* driver, had no effect on hemocyte numbers (Fig. 9A and B). However, it should be noted that the hemocyte proliferation phenotype with the fat body specific Lime overexpression was not as strong as with *Srp-Gal4* driver that is active both in the fat body and all hemocytes (Fig. 4D). The decrease in the number of circulating cells and the smaller size of the lymph gland observed in the Lime mutant could be rescued by the specific expression of Lime in the fat body using the *C7-Gal4* driver (Fig. 9C). We conclude that Lime expression in the fat body is responsible for the development of hemocytes both within the lymph gland and in circulation. Whether the fat body specific effect observed is due to changes in fat body mediated metabolic homeostasis or, for example, changes in fat body mediated systemic insulin signalling remains to be investigated.

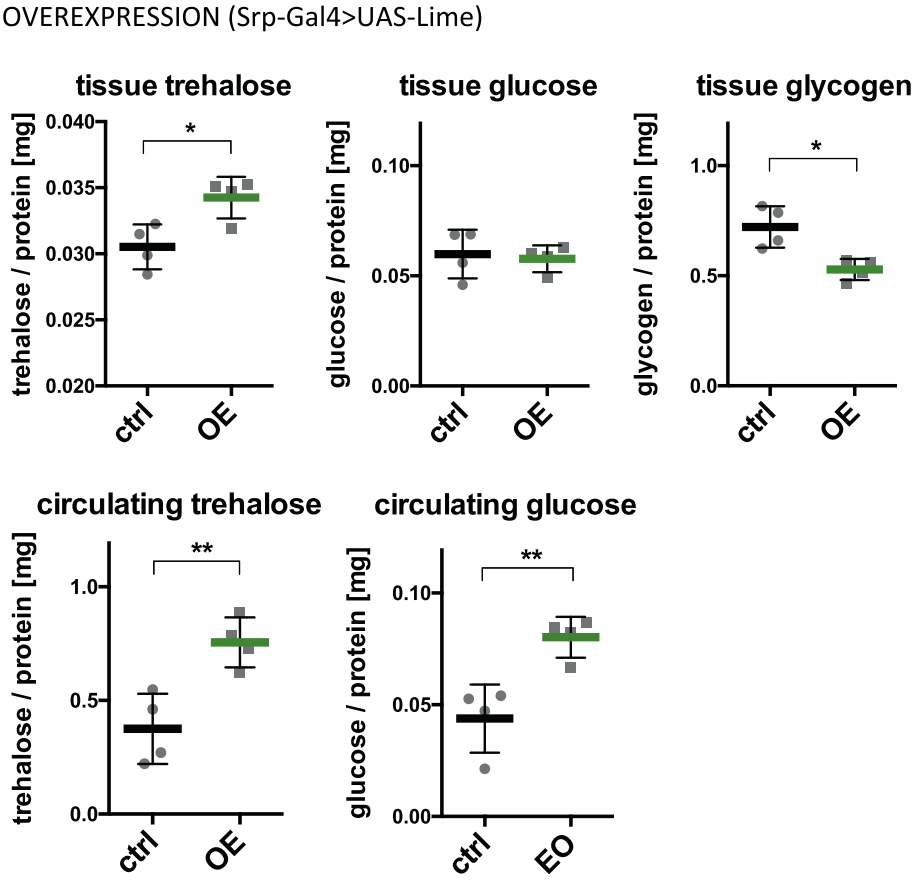

Fig. 8. Lime overexpression in hemocytes and fat body using *Srp-Gal4* leads to increased levels of circulating carbohydrates at the expense of stored glycogen. Analysis of trehalose, glucose and glycogen concentrations in the whole larva and in the hemolymph of larvae with Lime overexpression in hemocytes and fat body (*Srp-Gal4, UAS-Gal80^{ts} > UAS-Lime*, in green) and control (*Srp-Gal4, UAS-Gal80^{ts} > UAS-GFP,* in black) 24 h after wasp infection (inf), 96 h after egg laying. Mean with 95% confidence interval from 4 biological replicates.

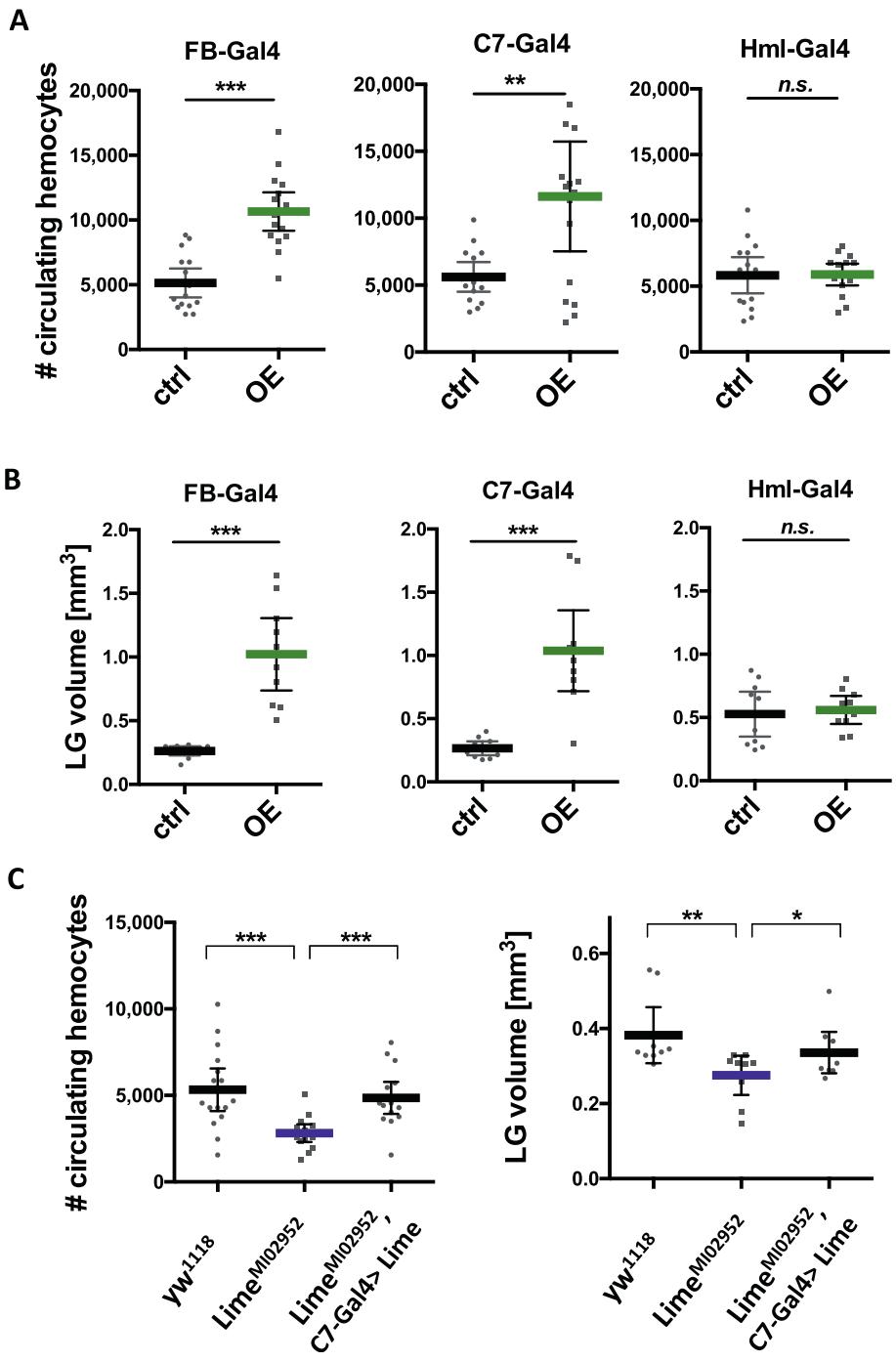

Fig. 9. Lime in the fat body regulates the number of circulating hemocytes and the size of lymph glands during larval development. A. Quantification of total number of circulating hemocytes after Lime over-expression in the fat body using *FB-Gal4* and *C7-Gal4* drivers and in the differentiated hemocytes using *Hml-Gal4* driver (in green). Mean with 95% confidence interval using 15 larvae per genotype. B. Quantification of the lymph gland volume after Lime over-expression in the fat body using *FB-Gal4* and *C7-Gal4* drivers and in the differentiated hemocytes using *Hml-Gal4* driver (in green). Mean with 95% confidence interval using 10 lymph glands per genotype. C. The number of circulating hemocytes and the size of the lymph glands in control (y^1w^{1118}), Lime mutant ($Lime^{MI02952}$, in blue) and in Lime mutant where the expression was driven in the fat body by *C7-Gal4* driver ($Lime^{MI02952}$, *C7-Gal4>UAS-Lime*). Mean with 95% confidence interval using 10 lymph glands per genotype.

4. Discussion

4.1. The role of Lime in hemocyte proliferation

We have found that Lime mutant larvae develop fewer immune cells, while over-expression of Lime leads to a dramatic expansion of undifferentiated prohemocytes in the lymph gland and in circulation (Figs. 3D and 4D). As Lime is normally expressed both in the immune cells and in the fat body, it is important to distinguish whether the effects on hemocyte proliferation, specification or function originate from an autonomous function of Lime in hemocytes or as a secondary effect of Lime mediated changes on systemic metabolism. It is interesting that the over-expression of Lime in the fat body leads to hemocyte expansion but that this phenotype is less profound than that when Lime is over-expressed both in the fat body and in hemocytes simultaneously; moreover, that the over-expression of Lime, solely within differentiated hemocytes does not affect hemocyte numbers at all (Figs. 4D and 9A). Importantly, expression of Lime within the fat body can rescue the low number of hemocytes in the Lime mutant (Fig. 9C). It therefore seems that the number of developing immune cells in the lymph gland and in circulation is actually influenced mainly by Lime in the fat body and the autonomous function of Lime within differentiated hemocytes is less important in this respect. Notwithstanding these assertions, the expression of Lime in hemocytes might still be needed during the immune challenge, either to regulate specification of immune cell types or to mediate signalling crosstalk between hemocytes and the fat body (or between hemocytes and other tissues involved in metabolic reprogramming). Indeed, in this respect it is interesting that Lime expression decreases in differentiating

lamellocytes (Fig. 6C). As we only investigated Lime expression in L3 larvae we cannot exclude the possibility that in the earlier phases of embryonic/larval development Lime is expressed also in the hemocyte progenitors where it stimulates their proliferation but its expression in the medullary zone disappears as the lymph gland matures. The *Srp > Lime* phenotype where we observe massive increase in prohemocyte population makes this a viable scenario, as the *Srp-Gal4* driver is active in both prohemocytes and hemocytes since the early embryonic development, including the embryonic hematopoetic primordium (Waltzer et al., 2003).

Autonomous effects on hemocyte proliferation have previously been observed by direct hemocyte activation of various signalling pathways; including the EGFR, Alk, Pvr, JNK, JAK/STAT, Toll, Hippo or TOR pathways (Zettervall et al., 2004) (Terriente-Felix et al., 2017) (Milton et al., 2014) (Dragojlovic-Munther and Martinez-Agosto, 2012). As we have not observe the formation of lamellocytes or melanotic masses under uninfected conditions, the Lime over-expression phenotype is reminiscent of that associated with EGFR receptor activation in circulating hemocytes (Zettervall et al., 2004), (Asha et al., 2003). The strongly impaired post-infection development of lamellocytes in Lime mutant would also be consistent with EGFR downregulation in plasmatocytes, as activation of EGFR is essential for lamellocyte formation after wasp infection (Sinenko et al., 2011). The giant lymph gland phenotype we observe in combination with Lime over-expression can not however be simply explained by autonomous EGFR over-activation (Dragojlovic-Munther and Martinez-Agosto, 2013), (Sinenko et al., 2011). Moreover, such a phenotype may involve Lime functioning in the signalling network between prohemocytes, differentiated cells and the PSC, for example via the activation of the JAK/STAT (Terriente-Felix et al., 2017) (Mondal et al., 2011), wg (Sinenko et al., 2009), Pvf1 (Mondal et al., 2014) or FGF pathways (Dragojlovic-Munther and Martinez-Agosto, 2013), or alternatively via the expression of Collier (Benmimoun et al., 2015) or ROS scavenging in the medullary zone (Owusu-Ansah and Banerjee, 2009). At the same time, the observed effects of both the Lime mutant and the Lime over-expression on hemocyte proliferation can simply be explained by Lime in the fat body affecting systemic metabolism and nutrient availability to the developing hemocytes.

As discussed, nutrient availability can profoundly influence immune cell differentiation and proliferation in the lymph gland. Larvae under prolonged starvation, exhibit smaller lymph glands with fewer prohemocytes and more differentiated cells (Dragojlovic-Munther and Martinez-Agosto, 2012) (Benmimoun et al., 2012) (Shim et al., 2012) (Tokusumi et al., 2012); a phenotype similar to that of the herein described Lime mutants. Starvation has also been shown to reduce the numbers of plasmatocytes in circulation (Yang and Hultmark, 2017), again consistent with our reported Lime mutants. Indeed, as the Lime mutant displays lower levels of circulating trehalose and low stores of glycogen and lipids, the effects on immune system we observe may be, at least partially, explained by the disturbed systemic metabolism.

4.2. The role of Lime during the immune response

The described Lime mutant exhibits a striking phenotype during the immune challenge provided by the infection of *Drosophila* larvae with the parasitic wasp *Leptopilina boulardii*. This is manifested in fewer circulating immune cells in the Lime mutant and the affected larvae failing to sustainably increase their hemocyte numbers during the infection response. Moreover, there is a concomitant failure to increase hemolymph glucose levels that are important during the immune defence (Bajgar et al., 2015), accompanied by impaired development of lamellocytes.

Both in the mammals and in vertebrates, the proliferation of hemocytes in mounting a successful immune defence is dependent on a temporal systemic metabolic switch, that preferentially allocates glucose to the circulating immune cells by inducing insulin resistance of the peripheral tissues (Straub et al., 2010) (Rauw, 2012). The metabolic switch after wasp infection is triggered by adenosine released from circulating hemocytes and involves inter-organ communication of hemocytes with the energy storing tissues (Bajgar et al., 2015). As we showed, the Lime mutant fails to up-regulate glucose levels in the circulation during the wasp infection (Fig. 6A) and this may significantly affect hemocyte proliferation and activation. While it is clear from our data that Lime mutant displays metabolic phenotype both before and after infection, it remains to be established if this is mediated through the Lime in the fat body or Lime in hemocytes and whether the metabolic changes involve inter-organ communication of hemocytes with energy regulating tissues, such as fat body or muscles.

Although the derived Lime mutants do not initially exhibit a deficiency to differentiate lamellocytes in the early stages of infection, there is a sharp drop in lamellocyte production from the 18 h after the infection (Fig. 6B). It is known that type I lamellocytes originate from hemocyte precursors and represent the prevailing type of lamellocytes developed as a response to wasp infection, as opposed to type II lamellocytes that trans-differentiate from plasmatocytes and are in minority (Anderl et al., 2016). Our experiments do not allow us to distinguish between these lamellocyte sub-types but we do detect fewer hemocyte progenitors in the Lime mutant. It is therefore possible that the lamellocytes observed during the first 18 h of infection may have their origin in the differentiation of hemocyte precursor and depletion of this pool of hemocyte progenitors might be responsible for the sudden decline of lamellocyte production observed in later stages of infection, despite the continued presence of plasmatocytes.

In summary, the Lime gene is expressed both in the hemocytes and in the fat body and it influences the development of hemocytes as well as the metabolic characteristics of the developing *Drosophila* larva. Moreover, energy expenditure as well as the development of the immune response is compromised in Lime mutant under the immune challenge. Although Lime mechanism of action still needs to be deciphered, it is clear that it simultaneosly regulates metabolism and immunity, well deserving its name.

Acknowledgement

We acknowledge the Bloomington Drosophila Stock Center and the Developmental Studies Hybridoma Bank for flies and antibodies and the BestGene and Genetic Services for fly injections. Special thanks to Sarah Bray in Cambridge where the work was started and funded by the Medical Research Council (MRC) Programme Grant G0800034. We thank Ales Tomcala for lipidomic MS data analysis. The project was funded by Czech Science Foundation (GACR) grant 17-17529S.

Appendix A. Supplementary data

Supplementary data to this article can be found online at https://doi.org/10.1016/j.ydbio.2019.05.005.

References

Anderl, I., Vesala, L., Ihalainen, T.O., Vanha-Aho, L.M., Ando, I., Ramet, M., Hultmark, D., 2016. Transdifferentiation and proliferation in two distinct hemocyte lineages in Drosophila melanogaster larvae after wasp infection. PLoS Pathog. 12 (7), e1005746.

Arrese, E.L., Wells, M.A., 1997. Adipokinetic hormone-induced lipolysis in the fat body of an insect, Manduca sexta: synthesis of sn-1,2-diacylglycerols. J. Lipid Res. 38 (1), 68–76.

Asha, H., Nagy, I., Kovacs, G., Stetson, D., Ando, I., Dearolf, C.R., 2003. Analysis of Ras-induced overproliferation in Drosophila hemocytes. Genetics 163 (1), 203–215.

Bajgar, A., Kucerova, K., Jonatova, L., Tomcala, A., Schneedorferova, I., Okrouhlik, J., Dolezal, T., 2015. Extracellular adenosine mediates a systemic metabolic switch during immune response. PLoS Biol. 13 (4), e1002135.

Benmimoun, B., Polesello, C., Waltzer, L., Haenlin, M., 2012. Dual role for Insulin/TOR signaling in the control of hematopoietic progenitor maintenance in Drosophila. Development 139 (10), 1713–1717.

Benmimoun, B., Polesello, C., Haenlin, M., Waltzer, L., 2015. The EBF transcription factor Collier directly promotes Drosophila blood cell progenitor maintenance independently of the niche. Proc. Natl. Acad. Sci. U. S. A. 112 (29), 9052–9057.

Buck, M.D., Sowell, R.T., Kaech, S.M., Pearce, E.L., 2017. Metabolic instruction of immunity. Cell 169 (4), 570–586.
Buttgereit, F., Burmester, G.R., Brand, M.D., 2000. Bioenergetics of immune functions: fundamental and therapeutic aspects. Immunol. Today 21 (4), 192–199.
Clark, R.I., Tan, S.W., Pean, C.B., Roostalu, U., Vivancos, V., Bronda, K., Pilatova, M., Fu, J., Walker, D.W., Berdeaux, R., et al., 2013. MEF2 is an in vivo immune-metabolic switch. Cell 155 (2), 435–447.
Corona, D.F., Armstrong, J.A., Tamkun, J.W., 2004. Genetic and cytological analysis of Drosophila chromatin-remodeling factors. Methods Enzymol. 377, 70–85.
Coustau, C., Carkion, Y., Nappi, A., Shotkoski, F., ffrench-Constant, R., 1996. Differential induction of antibacterial transcripts in Drosophila susceptible and resistant to parasitism by Leptopilina boulardi. Insect Mol. Biol. 5 (3), 167–172.
Delmastro-Greenwood, M.M., Piganelli, J.D., 2013. Changing the energy of an immune response. Afr. J. Clin. Exp. Immunol. 2 (1), 30–54.
DiAngelo, J.R., Bland, M.L., Bambina, S., Cherry, S., Birnbaum, M.J., 2009. The immune response attenuates growth and nutrient storage in Drosophila by reducing insulin signaling. Proc. Natl. Acad. Sci. U. S. A. 106 (49), 20853–20858.
Dragojlovic-Munther, M., Martinez-Agosto, J.A., 2012. Multifaceted roles of PTEN and TSC orchestrate growth and differentiation of Drosophila blood progenitors. Development 139 (20), 3752–3763.
Dragojlovic-Munther, M., Martinez-Agosto, J.A., 2013. Extracellular matrix-modulated Heartless signaling in Drosophila blood progenitors regulates their differentiation via a Ras/ETS/FOG pathway and target of rapamycin function. Dev. Biol. 384 (2), 313–330.
Folch, J., Lees, M., Sloane Stanley, G.H., 1957. A simple method for the isolation and purification of total lipides from animal tissues. J. Biol. Chem. 226 (1), 497–509.
Foley, E., O'Farrell, P.H., 2003. Nitric oxide contributes to induction of innate immune responses to gram-negative bacteria in Drosophila. Genes Dev. 17 (1), 115–125.
Gold, K.S., Bruckner, K., 2014. Drosophila as a model for the two myeloid blood cell systems in vertebrates. Exp. Hematol. 42 (8), 717–727.
Housden, B.E., Fu, A.Q., Krejci, A., Bernard, F., Fischer, B., Tavare, S., Russell, S., Bray, S.J., 2013. Transcriptional dynamics elicited by a short pulse of notch activation involves feed-forward regulation by E(spl)/Hes genes. PLoS Genet. 9 (1), e1003162.
Jenne, C.N., Kubes, P., 2013. Immune surveillance by the liver. Nat. Immunol. 14 (10), 996–1006.
Krejci, A., Bernard, F., Housden, B.E., Collins, S., Bray, S.J., 2009. Direct response to Notch activation: signaling crosstalk and incoherent logic. Sci. Signal. 2 (55), ra1.
Krzemien, J., Dubois, L., Makki, R., Meister, M., Vincent, A., Crozatier, M., 2007. Control of blood cell homeostasis in Drosophila larvae by the posterior signalling centre. Nature 446 (7133), 325–328.
Krzemien, J., Oyallon, J., Crozatier, M., Vincent, A., 2010. Hematopoietic progenitors and hemocyte lineages in the Drosophila lymph gland. Dev. Biol. 346 (2), 310–319.
Kuhnlein, R.P., 2012. Thematic review series: lipid droplet synthesis and metabolism: from yeast to man. Lipid droplet-based storage fat metabolism in Drosophila. J. Lipid Res. 53 (8), 1430–1436.
Leitao, A.B., Sucena, E., 2015. Drosophila sessile hemocyte clusters are true hematopoietic tissues that regulate larval blood cell differentiation. Elife 4.
Letourneau, M., Lapraz, F., Sharma, A., Vanzo, N., Waltzer, L., Crozatier, M., 2016. Drosophila hematopoiesis under normal conditions and in response to immune stress. FEBS Lett. 590 (22), 4034–4051.
Levy, M., Thaiss, C.A., Elinav, E., 2016. Metabolites: messengers between the microbiota and the immune system. Genes Dev. 30 (14), 1589–1597.
Man, K., Kutyavin, V.I., Chawla, A., 2017. Tissue immunometabolism: development, physiology, and pathobiology. Cell Metabol. 25 (1), 11–26.
Mandal, L., Martinez-Agosto, J.A., Evans, C.J., Hartenstein, V., Banerjee, U., 2007. A Hedgehog- and Antennapedia-dependent niche maintains Drosophila haematopoietic precursors. Nature 446 (7133), 320–324.
Mathis, D., 2013. Immunological goings-on in visceral adipose tissue. Cell Metabol. 17 (6), 851–859.
Merenciano, M., Ullastres, A., de Cara, M.A., Barron, M.G., Gonzalez, J., 2016. Multiple independent retroelement insertions in the promoter of a stress response gene have variable molecular and functional effects in Drosophila. PLoS Genet. 12 (8), e1006249.
Milton, C.C., Grusche, F.A., Degoutin, J.L., Yu, E., Dai, Q., Lai, E.C., Harvey, K.F., 2014. The Hippo pathway regulates hematopoiesis in Drosophila melanogaster. Curr. Biol. 24 (22), 2673–2680.
Mondal, B.C., Mukherjee, T., Mandal, L., Evans, C.J., Sinenko, S.A., Martinez-Agosto, J.A., Banerjee, U., 2011. Interaction between differentiating cell- and niche-derived signals in hematopoietic progenitor maintenance. Cell 147 (7), 1589–1600.
Mondal, B.C., Shim, J., Evans, C.J., Banerjee, U., 2014. Pvr expression regulators in equilibrium signal control and maintenance of Drosophila blood progenitors. Elife 3, e03626.
Okamoto, N., Yamanaka, N., Yagi, Y., Nishida, Y., Kataoka, H., O'Connor, M.B., Mizoguchi, A., 2009. A fat body-derived IGF-like peptide regulates postfeeding growth in Drosophila. Dev. Cell 17 (6), 885–891.
Owusu-Ansah, E., Banerjee, U., 2009. Reactive oxygen species prime Drosophila haematopoietic progenitors for differentiation. Nature 461 (7263), 537–541.
Rauw, W.M., 2012. Immune response from a resource allocation perspective. Front. Genet. 3, 267.
Rizki, T.M., Rizki, R.M., 1992. Lamellocyte differentiation in Drosophila larvae parasitized by Leptopilina. Dev. Comp. Immunol. 16 (2–3), 103–110.
Roth, S.W., Bitterman, M.D., Birnbaum, M.J., Bland, M.L., 2018. Innate immune signaling in Drosophila blocks insulin signaling by uncoupling PI(3,4,5)P3 production and akt activation. Cell Rep. 22 (10), 2550–2556.
Sarov, M., Barz, C., Jambor, H., Hein, M.Y., Schmied, C., Suchold, D., Stender, B., Janosch, S., JV, K., Krishnan, R.T., et al., 2016. A genome-wide resource for the analysis of protein localisation in Drosophila. Elife 5, e12068.
Schmid, M.R., Anderl, I., Vesala, L., Vanha-aho, L.M., Deng, X.J., Ramet, M., Hultmark, D., 2014. Control of Drosophila blood cell activation via Toll signaling in the fat body. PLoS One 9 (8), e102568.
Schneedorferova, I., Tomcala, A., Valterova, I., 2015. Effect of heat treatment on the n-3/n-6 ratio and content of polyunsaturated fatty acids in fish tissues. Food Chem. 176, 205–211.
Shia, A.K., Glittenberg, M., Thompson, G., Weber, A.N., Reichhart, J.M., Ligoxygakis, P., 2009. Toll-dependent antimicrobial responses in Drosophila larval fat body require Spatzle secreted by haemocytes. J. Cell Sci. 122 (Pt 24), 4505–4515.
Shim, J., Mukherjee, T., Banerjee, U., 2012. Direct sensing of systemic and nutritional signals by haematopoietic progenitors in Drosophila. Nat. Cell Biol. 14 (4), 394–400.
Sinenko, S.A., Mathey-Prevot, B., 2004. Increased expression of Drosophila tetraspanin, Tsp68C, suppresses the abnormal proliferation of ytr-deficient and Ras/Raf-activated hemocytes. Oncogene 23 (56), 9120–9128.
Sinenko, S.A., Mandal, L., Martinez-Agosto, J.A., Banerjee, U., 2009. Dual role of wingless signaling in stem-like hematopoietic precursor maintenance in Drosophila. Dev. Cell 16 (5), 756–763.
Sinenko, S.A., Shim, J., Banerjee, U., 2011. Oxidative stress in the haematopoietic niche regulates the cellular immune response in Drosophila. EMBO Rep. 13 (1), 83–89.
Spiljar, M., Merkler, D., Trajkovski, M., 2017. The immune system bridges the gut microbiota with systemic energy homeostasis: focus on TLRs, mucosal barrier, and SCFAs. Front. Immunol. 8, 1353.
Straub, R.H., Cutolo, M., Buttgereit, F., Pongratz, G., 2010. Energy regulation and neuroendocrine-immune control in chronic inflammatory diseases. J. Intern. Med. 267 (6), 543–560.
Tennessen, J.M., Barry, W.E., Cox, J., Thummel, C.S., 2014. Methods for studying metabolism in Drosophila. Methods 68 (1), 105–115.
Terriente-Felix, A., Perez, L., Bray, S.J., Nebreda, A.R., Milan, M., 2017. A Drosophila model of myeloproliferative neoplasm reveals a feed-forward loop in the JAK pathway mediated by p38 MAPK signalling. Dis Model Mech 10 (4), 399–407.
Thibault, S.T., Singer, M.A., Miyazaki, W.Y., Milash, B., Dompe, N.A., Singh, C.M., Buchholz, R., Demsky, M., Fawcett, R., Francis-Lang, H.L., et al., 2004. A complementary transposon tool kit for Drosophila melanogaster using P and piggyBac. Nat. Genet. 36 (3), 283–287.
Tokusumi, Y., Tokusumi, T., Shoue, D.A., Schulz, R.A., 2012. Gene regulatory networks controlling hematopoietic progenitor niche cell production and differentiation in the Drosophila lymph gland. PLoS One 7 (7), e41604.
Venken, K.J., Schulze, K.L., Haelterman, N.A., Pan, H., He, Y., Evans-Holm, M., Carlson, J.W., Levis, R.W., Spradling, A.C., Hoskins, R.A., et al., 2011. MiMIC: a highly versatile transposon insertion resource for engineering Drosophila melanogaster genes. Nat. Methods 8 (9), 737–743.
Vlisidou, I., Wood, W., 2015. Drosophila blood cells and their role in immune responses. FEBS J. 282 (8), 1368–1382.
Waltzer, L., Ferjoux, G., Bataille, L., Haenlin, M., 2003. Cooperation between the GATA and RUNX factors serpent and lozenge during Drosophila hematopoiesis. EMBO J. 22 (24), 6516–6525.
Yamada, T., Habara, O., Kubo, H., Nishimura, T., 2018. Fat body glycogen serves as a metabolic safeguard for the maintenance of sugar levels in Drosophila. Development 145 (6).
Yang, H., Hultmark, D., 2017. Drosophila muscles regulate the immune response against wasp infection via carbohydrate metabolism. Sci. Rep. 7 (1), 15713.
Zettervall, C.J., Anderl, I., Williams, M.J., Palmer, R., Kurucz, E., Ando, I., Hultmark, D., 2004. A directed screen for genes involved in Drosophila blood cell activation. Proc. Natl. Acad. Sci. U. S. A. 101 (39), 14192–14197.
Zhang, Y., Xi, Y., 2015. Fat body development and its function in energy storage and nutrient sensing in Drosophila melanogaster. J. Tissue Sci. Eng. 6 (1), 141.
Zmora, N., Bashiardes, S., Levy, M., Elinav, E., 2017. The role of the immune system in metabolic health and disease. Cell Metabol. 25 (3), 506–521.